Full counting statistics in the gapped XXZ spin chain

Pasquale Calabrese[1,2,3], Mario Collura[1], Giuseppe Di Giulio[1,2] and Sara Murciano[1,2]

[1] *International School for Advanced Studies (SISSA), via Bonomea 265, 34136 Trieste, Italy*
[2] *INFN, sezione di Trieste, via Bonomea 265, 34136 Trieste, Italy*
[3] *International Centre for Theoretical Physics (ICTP), I-34151, Trieste, Italy*

*** Missing PACS ***

Abstract – We exploit the knowledge of the entanglement spectrum in the ground state of the gapped XXZ spin chain to derive asymptotic exact results for the full counting statistics of the transverse magnetisation in a large spin block of length ℓ. We found that for a subsystem of even length the full counting statistics is Gaussian, while for odd subsystems it is the sum of *two* Gaussian distributions. We test our analytic predictions with accurate tensor networks simulations. As a byproduct, we also obtain the symmetry (magnetisation) resolved entanglement entropies.

Introduction. – The process of measurement in quantum mechanics is intrinsically probabilistic: the measure of a given observable generically provides different outcomes in identically prepared systems. Hence, the probability distribution (PDF) of an observable is a natural quantity to consider in any quantum mechanical system and provides much more information than the average value of the same observable. In many-body systems, these PDFs, or equivalently their full counting statistics (FCS), have been the subject of intensive investigations since many years with a focus mainly on local observables (i.e. defined in a given point or lattice site) or global ones (i.e. extensive quantities involving the entire system). Only in recent time, the attention shifted to observables with support on a finite, but large, subsystem embedded in a thermodynamic one, partially motivated by some cold atomic experiments [1–6] and by the connection with the entanglement entropy of the same subsystem [7–16]. In spite of a large recent literature on the subject [17–41], results based on integrability for one-dimensional exactly solvable *interacting* models are still scarse (see [30,31]).

In this Letter, we provide an explicit exact calculation for the PDF and for the FCS of an observable within an extended subsystem. We consider the ground state of the XXZ spin chain defined by the Hamiltonian

$$H_{\rm XXZ} = \sum_j \left[\sigma_j^x\sigma_{j+1}^x + \sigma_j^y\sigma_{j+1}^y + \Delta\sigma_j^z\sigma_{j+1}^z\right], \qquad (1)$$

where σ_j^α, $\alpha = x, y, z$ are the Pauli matrices at site j. We focus in the antiferromagnetic gapped regime with $\Delta > 1$. The observable of interest is the transverse magnetisation for a block of ℓ contiguous spins, i.e.

$$S_\ell^z = \frac{1}{2}\sum_{j=1}^{\ell}\sigma_j^z. \qquad (2)$$

In particular, since the total transverse magnetisation $(\sum_j \sigma_j^z/2)$ is conserved, the FCS can be directly obtained from the entanglement spectrum of the subsystem. Indeed, the reduced density matrix ρ_ℓ of the subsystem is organised in blocks of fixed magnetisation (quantised in terms of integers or half-integers up to $\ell/2$ depending on the parity of ℓ). In order to work with an observable with integer eigenvalues for any ℓ, it is convenient to focus on the difference of the block magnetisation with the Néel state, i.e.

$$\delta S_\ell^z \equiv \sum_{j=1}^{\ell}\left(\frac{\sigma_j^z}{2} - \frac{(-1)^j}{2}\right). \qquad (3)$$

The probability of a measurement of the subsystem magnetisation with outcome $\delta S_\ell^z = q$ is just the trace of the block of ρ_ℓ in the sector with $\delta S^z = q$, i.e.

$$P(q) = {\rm Tr}\rho_\ell\Pi_q = \sum_{s\,\in\,\mathcal{S}_q}\lambda_s\,, \qquad (4)$$

where Π_q is the projector on the sector of magnetisation $\delta S^z = q$, λ_s are the eigenvalues of ρ_ℓ, and $\mathcal{S}_q$ stands for all the eigenvalues in that magnetisation sector (notice that $\sum_q P(q) = {\rm Tr}\rho_\ell = 1$ by construction). Similarly the FCS

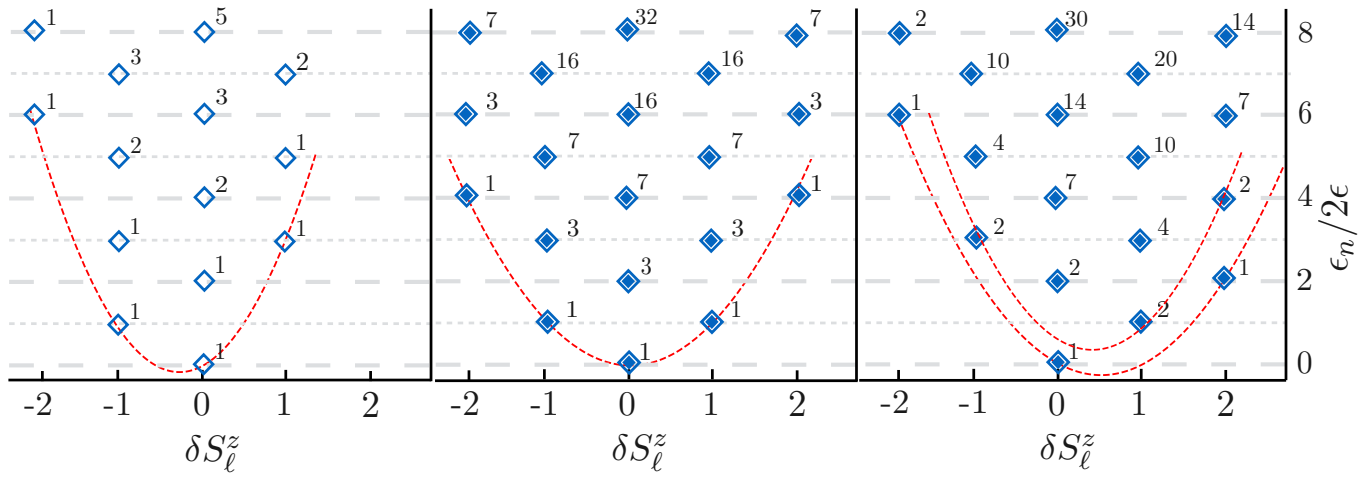

Fig. 1: Entanglement spectra of the gapped XXZ spin chain in the three configurations we consider here. Left: Semi-infinite line. Center: A block of ℓ contiguous spins with ℓ even. Right: A block with ℓ odd. We report the logarithm of the eigenvalues of the reduced density matrix ϵ_n in units of 2ϵ, with $\epsilon = \text{arccosh}\Delta$, as function of δS^z_ℓ (cf. (3)). Each tilted square signals the presence of an eigenvalue with degeneracy given by the nearby number. The dashed-red parabolas are envelopes of the location of the largest eigenvalue of the RDM at fixed δS^z_ℓ. Notice that in the left and in the center, the towers of degeneracies are independent of δS^z_ℓ. Conversely, on the right, i.e. for odd blocks, there are two towers depending on the parity of δS^z_ℓ.

generating function is defined as

$$G(\lambda) \equiv \text{Tr}\rho_\ell e^{i\lambda\delta S^z_\ell} = \sum_q P(q) e^{iq\lambda}; \tag{5}$$

its derivatives in $\lambda = 0$ provide the moments of the observables δS^z_ℓ. Hence the exact knowledge of the entanglement spectrum also provides the FCS of the total transverse magnetisation (in general it provides the FCS of any conserved charge). For the ground state of the XXZ spin chain in the gapped regime, the entanglement spectrum has been obtained in Ref. [42]. We exploit its knowledge here to reconstruct the PDF and the FCS of the subsystem magnetisation.

The remaining of this Letter is organised as follows. First, we recap and generalise results for the entanglement spectrum of Ref. [42]. Then we reconstruct the PDF and the FCS for both even and odd number of sites of the subsystem. As a byproduct, we also derive some results for the symmetry resolved entanglement. Finally we draw our conclusions.

Recap on the entanglement spectrum. – We consider the symmetry broken ground state, i.e. the one that for large Δ converges to the Néel state. This state is doubly degenerate, so there are two equivalent states which are mapped into each other by the translation of one site. Let us first consider the case of $\ell = \infty$, i.e. the subsystem being the semi-infinite line. In this case, the logarithm of the eigenvalues of ρ_ℓ are equispaced, i.e. $\lambda_s = e^{-\epsilon_s}$ with $\epsilon_s = 2\epsilon s$, where $\epsilon = \text{arccosh}\Delta$ (see, e.g., [43, 44]). The total degeneracy $D_{\rm h}(s)$ of the level $2\epsilon s$ is the number of partitions of s into smaller non-repeated integers (including zero). Here we need to know how these eigenvalues distribute among sectors of fixed magnetisation; this has been worked out in [42] with a combination of perturbation theory and integrability arguments. The first panel of Figure 1 reports the structure of the entanglement spectrum based on the results of Ref. [42]. The final result for the degeneracy of the eigenvalue with $\delta S^z_\ell = q$ at level s is $d_{\rm h}(q,s) = p_{\rm h}(\frac{s-m_{\rm h}(q)}{2})$ [42], with $p_{\rm h}(n)$ the number of integer partitions of n and $m_{\rm h}(q) = q(2q+1)$. We use the convention that $p_{\rm h}(x) = 0$ for negative integers and for half-integers. (The other degenerate state –sometimes called Antineel for $\Delta \to \infty$– is obtained by sending $q \to -q$ with the net effect of having $m_{\rm a}(q) = q(2q-1)$.) The number of partitions $p_{\rm h}(x)$ has not an analytic form; the same is true for the total degeneracy $D_{\rm h}(x)$ above; however both have simple generating functions given by

$$\sum_{s=0} p_{\rm h}(s)x^s = \prod_{k=1}^{\infty} \frac{1}{1-x^k}, \qquad \sum_{s=0} D_{\rm h}(s)y^s = \prod_{k=1}^{\infty}(1+y^k). \tag{6}$$

Notice that the degeneracies of the various sectors are all the same, there is only an overall shift of the lowest eigenvalues at fixed q given by $m_{\rm h}(q)$. Recalling that the PDF $P(q)$ is just the sum of all the eigenvalues of the RDM at fixed q (weighted with their degeneracy), this is the same for all q except for the important factor of the largest eigenvalue at fixed q equal to $e^{-2\epsilon m_{\rm h}(q)}$. Hence the PDF is just

$$P_{\rm h}(q) = \mathcal{N} e^{-2\epsilon q(2q+1)}, \quad \text{with } \mathcal{N}^{-1} = \theta_3\left(i\epsilon, e^{-4\epsilon}\right), \tag{7}$$

and indeed it was already obtained in Ref. [46] (here θ_3 is the elliptic theta function).

Now, still following the approach of Ref. [42], we explain how to use these results to obtain the entanglement spectrum of a finite large interval. As long as ℓ is larger than the correlation length, the reduced density matrix ρ_ℓ of a single interval with two boundaries factorises into $\rho_L \otimes \rho_R$, where $\rho_{L/R}$ are the reduced density matrices for the semi-infinite lines having the left/right end-point of the interval. The combination of these two spectra into a single one is graphically reported in Fig. 1. We show both cases for even and odd subsystems (center and right respectively). For an even subsystem we should combine two different spectra $m_L(x) = m_{\rm h}(x) = x(2x+1)$ and $m_R(x) = m_{\rm a}(x) = x(2x-1)$ from left and right. Conversely, for odd blocks, the left and the right spectra to combine are equal, e.g. $m_L(x) = m_R(x) = x(2x+1)$. The final results for the degeneracies are reported in the figure. In the even case, we have that the degeneracy at fixed q at level s can be written as $d_{\rm e}(q,s) = p_{\rm e}(\frac{s-m_{\rm e}(q)}{2})$ with $m_{\rm e}(q) = q^2$ and $p_{\rm e}$ generated by

$$\sum_{s=0} p_{\rm e}(s) x^s = \prod_{k\geq 1} \frac{(1+x^k)^2}{1-x^k}\,, \tag{8}$$

leading to the generating function for the total degeneracy $D_{\rm e}(s)$ of level s

$$\sum_{s=0} D_{\rm e}(s) x^s = \prod_{k\geq 1} (1+x^k)^2. \tag{9}$$

Notice that while the generating function for $D_{\rm e}(s)$ is the square of the one for $D_{\rm h}(s)$, the same is not true for $p_{\rm e}$. Again we employ the convention $p_{\rm e}(x) = 0$ for negative numbers and for half-integers.

For odd blocks, it is more complicated to combine the two spectra for even and odd q. The degeneracies of both sectors have the generating function

$$\sum_{s=0} p^{\rm b}_{\rm o}(s) x^s = \prod_{k\geq 1} \frac{(1-x^{2k})^3}{(1-x^k)^2(1-x^{4k})^2}, \tag{10}$$

where even (odd) powers of x correspond to even (odd) values of q. However, a single generating function for different q is not a too useful tool to write symmetry resolved quantities. Exploiting some identities of elliptic theta functions $\theta_{2,3}$, we can extract the even and the odd part of (10) we are interested in. After some algebra we get (for $x>0$)

$$\sum_{s=0} p_{\rm o}(s,q) x^s = \frac{(\theta_2(x^4))^{\frac{1-(-1)^q}{2}} (\theta_3(x^4))^{\frac{1+(-1)^q}{2}}}{\prod_{k\geq 1}(1+x^{2k})(1-(-x)^k)(1-x^k)}, \tag{11}$$

which does depend on the parity of q. Hence the degeneracy of the level s with fixed q is

$$d_{\rm o}(q,s) = p_{\rm o}(s - m_{\rm o}(q)), \tag{12}$$

with $m_{\rm o}(q) = q^2 - q$. Indeed $m_{\rm o}(q)$ and $m_{\rm o}(q)+1$ are the two parabolas in Fig. 1, envelopes of the largest eigenvalues of the RDM for even and odd q respectively. The generating function for the total degeneracy $D_{\rm o}(s)$ of level s is the same as $D_{\rm e/h}(s)$ in Eq. (9).

Full counting statistics: even number of sites. – The easiest way to get the PDF $P_{\rm e}(q)$ for the interval is to combine the PDFs at the right and left boundary as

$$P_{\rm e} = \sum_{q_1=-\infty}^{\infty} P_L(q_1) P_R(q-q_1) = \sum_{q_1=-\infty}^{\infty} P_{\rm h}(q_1) P_{\rm h}(q_1-q), \tag{13}$$

where we used that the PDF at the two boundaries are $P_L(q) = P_{\rm h}(q_1)$ and $P_R(q) = P_{\rm h}(-q)$. The sum is easily rewritten as

$$P_{\rm e}(q) = \mathcal{N}^2 e^{-2\epsilon(q^2-1/4)} \sum_{q_1=-\infty}^{\infty} e^{-2\epsilon(2q_1+q+1/2)^2}. \tag{14}$$

The remaining sum over q_1 does not depend on q, for integer q. Hence the PDF is Gaussian

$$P_{\rm e}(q) = \mathcal{N}_{\rm e} e^{-2q^2\epsilon}, \tag{15}$$

and the normalisation factor is $\mathcal{N}_{\rm e}^{-1} = \sum_q e^{-2q^2\epsilon} = \theta_3(e^{-2\epsilon})$. The FCS is the Fourier series (5) which immediately leads to

$$G_{\rm e}(\lambda) = \frac{\theta_3\left(\frac{\lambda}{2}, e^{-2\epsilon}\right)}{\theta_3(e^{-2\epsilon})}. \tag{16}$$

Notice that this is real and even in λ. As a cross check, the same result is re-obtained by directly summing over the eigenvalues of the RDM with the degeneracies reported in Fig. 1 (to perform the sum, one exploits (8) the product representation of the θ_3 function).

The FCS generating function is directly measured in iTEBD simulations [45], as explained in details, e.g., in Refs. [27, 37]. The results in the thermodynamic limit for three values of $\Delta > 1$ and for $\ell = 200$ are shown in Figure 2. The agreement is always excellent (data and predictions are superimposed) for all considered values of Δ. We mention that as Δ gets close to 1, one should consider much larger values of ℓ to reach such good agreement due to the diverging correlation length at the isotropic point.

Full counting statistics: odd number of sites. – Also for this case, the PDF can be obtained combining two single-boundary ones as

$$P_{\rm o} = \sum_{q_1=-\infty}^{\infty} P_L(q_1) P_R(q-q_1) = \sum_{q_1=-\infty}^{\infty} P_{\rm h}(q_1) P_{\rm h}(q-q_1), \tag{17}$$

where we used that the PDF at the two boundaries are the same. Again, the sum is easily rewritten as

$$P_{\rm o}(q) = \mathcal{N}^2 e^{-2\epsilon(q^2-q)} \sum_{q_1=-\infty}^{\infty} e^{-2\epsilon(2q_1-q)^2}. \tag{18}$$

However, this time the remaining sum *does* depend on the parity of q. Performing this sum, the PDF is

$$P_{\rm o}(q) = \mathcal{N}_{\rm o} e^{-2\epsilon(q^2-q)} \times \begin{cases} \theta_3(e^{-8\epsilon}), & q \text{ even}, \\ \theta_2(e^{-8\epsilon}), & q \text{ odd}, \end{cases} \tag{19}$$

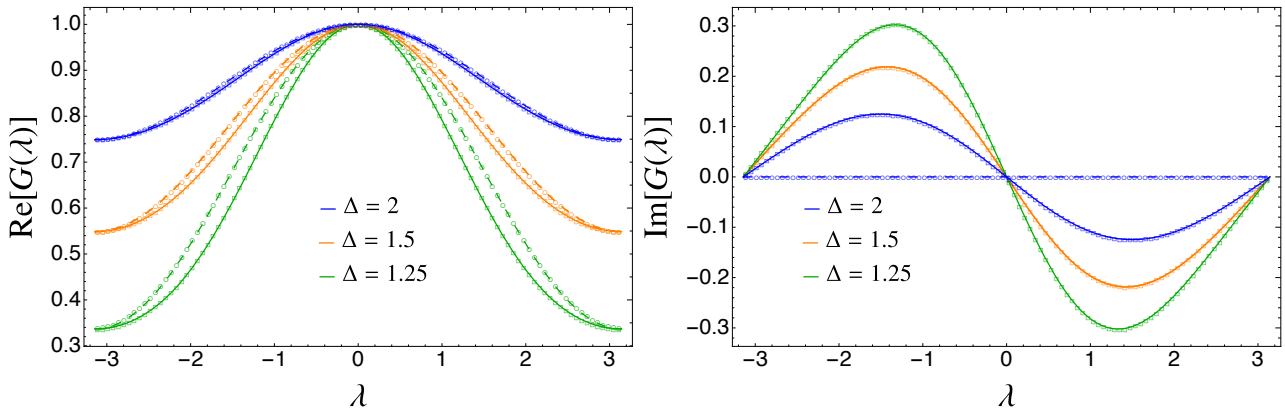

Fig. 2: Full counting statistics generating functions $G(\lambda)$ for the gapped XXZ spin chain for three values of Δ. The left (right) panel is the real (imaginary) part of $G(\lambda)$. The symbols are the iTEBD data that perfectly match the superimposed analytic predictions (full lines for odd ℓ and dashed for even ℓ). The data are for infinite chains and subsystems equal to $\ell = 200$ (circles) or 201 (squares). Notice that the real parts for even and odd q are qualitatively similar, but quantitatively different.

with $\mathcal{N}_0$ easily obtained from the normalisation.

The FCS is the Fourier series (5) which, after some manipulations using the properties of elliptic functions, leads to

$$G_{\rm o}(\lambda) = \left(\frac{\theta_3\left(i\epsilon - \frac{\lambda}{2}, e^{-4\epsilon}\right)}{\theta_3(i\epsilon, e^{-4\epsilon})} \right)^2 . \tag{20}$$

Notice that this FCS has a non-vanishing and non-trivial imaginary part, but satisfy $G_{\rm o}(\lambda)^* = G_{\rm o}(-\lambda)$. Again, as a cross check, this result is re-obtained by directly summing over the eigenvalues of the RDM with the degeneracies reported in Fig. 1.

Also for odd ℓ, the analytical prediction (20) is tested against iTEBD simulations in Figure 2. In these simulations, we measure the FCS of the operator S^z_ℓ and not δS^z_ℓ; hence the numerical data have been divided by $e^{i\lambda/2}$. After this normalisation, the agreement between data and prediction is extremely good in all considered cases.

Byproduct: symmetry resolved entropies. – A very recent research line in many body quantum systems is to understand how the entanglement organises into the various symmetry sectors of a theory [46–56]. The reduced density matrix is symmetry decomposed as $\rho_\ell = \oplus_q P(q)\rho_\ell(q)$. The symmetry resolution of the entanglement spectrum reported in Figure 1 allows us to access the symmetry resolved moments as

$$\mathcal{Z}_n(q) \equiv \sum_{s\in\mathcal{S}_q} \lambda_s^n = \frac{\sum_j d(q,j) e^{-2n\epsilon j}}{\left(\sum_j D(j) e^{-2\epsilon j}\right)^n} , \tag{21}$$

where $d(q,j)$ and $D(j)$ are respectively the degeneracies of the j-th eigenvalue for fixed q and total (whose generating functions are known in the three cases of interest). The symmetry resolved entropies are defined as

$$S_n(q) \equiv \frac{1}{1-n} \ln {\rm Tr}\rho_\ell^n(q) = \frac{1}{1-n} \ln {\rm Tr} \frac{\mathcal{Z}_n(q)}{\mathcal{Z}_1^n(q)}. \tag{22}$$

Since in $S_n(q)$ only the ratio $\mathcal{Z}_n(q)/\mathcal{Z}_1^n(q)$ matters, the dependence on D_j cancels and

$$\frac{\mathcal{Z}_n(q)}{\mathcal{Z}_1^n(q)} = \frac{\sum_j d(q,j) e^{-2n\epsilon j}}{\left(\sum_j d(q,j) e^{-2\epsilon j}\right)^n} = \frac{\sum_j p(j) e^{-2an\epsilon j}}{\left(\sum_j p(j) e^{-2a\epsilon j}\right)^n}, \tag{23}$$

where in the last equality we used $d(q,s) = p(\frac{s-m(q)}{a})$ (with $a = 2$ for semi-infinite and even ℓ, while $a = 1$ for odd ℓ) and shifted the sum as $(j - m(q))/a \to j$ (notice that the actual value of $m(q)$ is unessential).

The result for the semi-infinite line has been already derived in Ref. [46] and we recall it here:

$$S_n^{\rm h}(q) = \frac{1}{1-n} \sum_{k=1}^{\infty} [n \ln(1 - e^{-4\epsilon k}) - \ln(1 - e^{-4n\epsilon k})], \tag{24}$$

as simply follows combining (23) with (6). Now we derive the entropies for a finite interval of both even and odd length. For even ℓ, the two sums in (23) can be rewritten in terms of generating functions (8) (with $x = e^{-4n\epsilon}$), obtaining

$$S_n^{\rm e}(q) = \frac{\displaystyle\sum_{k=1}^{\infty} \left[\ln \frac{(1+e^{-4n\epsilon k})^2}{1-e^{-4n\epsilon k}} - n \ln \frac{(1+e^{-4\epsilon k})^2}{1-e^{-4\epsilon k}} \right]}{1-n}. \tag{25}$$

Very importantly, the symmetry resolved entropies are *not the double* of the single resolved entropies (24) for the half line as it is the case for the total one (mathematically this is a consequence of the relation between the generating function for $D_{\rm e}(s)$ and $D_{\rm h}(s)$, but not for $p_{\rm e/h}$). Also, these symmetry resolved entanglement entropies are independent of q and hence satisfy the equipartition of entanglement [51] exactly.

In the very same fashion, we can repeat the calculation

for odd ℓ, obtaining the more cumbersome expression

$$S_n^{\rm o}(q) = \frac{1}{1-n}\Bigg[\sum_{k=1}^{\infty}\Bigg(n\ln(1+e^{-4\epsilon k})(1-e^{-2\epsilon k})(1-(-)^k e^{-2\epsilon k}) - \ln(1+e^{-4\epsilon nk})(1-e^{-2\epsilon nk})(1-(-)^k e^{-2\epsilon nk})\Bigg) + \frac{1+(-)^q}{2}(\ln\theta_3(e^{-8\epsilon n}) - n\ln\theta_3(e^{-8\epsilon}) + \frac{1-(-)^q}{2}(\ln\theta_2(e^{-8\epsilon n}) - n\ln\theta_2(e^{-8\epsilon})\Bigg], \quad (26)$$

Hence, for odd ℓ, the symmetry resolved entropies do depend on the parity of q and the equipartition of entanglement is explicitly broken.

We finally mention, as a highly non-trivial crosscheck, that it is possible, but cumbersome, to sum over the various sectors q in order to recover the total entanglement, both for even and odd ℓ. The calculation parallels the one for the half-line in [46].

Conclusions. – We computed the FCS of the transverse magnetisation in gapped XXZ chains within a spin block of length ℓ, for ℓ larger than the correlation length. Our main results are the exact formulas for the generating functions (16) and (20) valid for even and odd ℓ respectively. Their accuracy has been tested against iTEBD simulations, see Figure 2. The astonishing simplicity of the final results resides in the entanglement spectrum being equispaced, as reported in Figure 1. The symmetry resolved entanglement entropies turn out to be a simple byproduct of our results.

An extremely interesting open question is whether one can access the crossover from the conformal regime [18,19] (valid for $\ell \ll \xi$, with ξ being the correlation length) to massive one ($\ell \gg \xi$) we obtained here. It is likely that exact techniques developed for the entanglement entropy [57,58] may be used even for this problem.

* * *

We thank Fabian Essler for discussions. PC and SM acknowledge support from ERC under Consolidator grant number 771536 (NEMO).

REFERENCES

[1] J. Armijo, T. Jacqmin, K. V. Kheruntsyan, and I. Bouchoule, *Probing Three-Body Correlations in a Quantum Gas Using the Measurement of the Third Moment of Density Fluctuations*, Phys. Rev. Lett. **105**, 230402 (2010).

[2] T. Jacqmin, J. Armijo, T. Berrada, K. V. Kheruntsyan, and I. Bouchoule, *Sub-Poissonian Fluctuations in a 1D Bose Gas: From the Quantum Quasicondensate to the Strongly Interacting Regime*, Phys. Rev. Lett. **106**, 230405 (2011).

[3] S. Hofferberth, I. Lesanovsky, T. Schumm, A. Imambekov, V. Gritsev, E. Demler, and J. Schmiedmayer, *Probing quantum and thermal noise in an interacting many-body system*, Nature Phys. **4**, 489 (2008).

[4] T. Kitagawa, S. Pielawa, A. Imambekov, J. Schmiedmayer, V. Gritsev, and E. Demler, *Ramsey Interference in One-Dimensional Systems: The Full Distribution Function of Fringe Contrast as a Probe of Many-Body Dynamics*, Phys. Rev. Lett. **104**, 255302 (2010).

[5] T. Kitagawa, A. Imambekov, J. Schmiedmayer, and E. Demler, *The dynamics and prethermalization of one-dimensional quantum systems probed through the full distributions of quantum noise*, New J. Phys. **13**, 73018 (2011).

[6] M. Gring, M. Kuhnert, T. Langen, T. Kitagawa, B. Rauer, M. Schreitl, I. Mazets, D. A. Smith, E. Demler, and J. Schmiedmayer, *Relaxation and Prethermalization in an Isolated Quantum System*, Science **337**, 1318 (2012).

[7] I. Klich and L. Levitov, *Quantum Noise as an Entanglement Meter*, Phys. Rev. Lett. **102**, 100502 (2009).

[8] I. Klich and L. Levitov, *Many-Body Entanglement: a New Application of the Full Counting Statistics*, Adv. Theor. Phys. **1134**, 36 (2009).

[9] B. Hsu, E. Grosfeld, and E. Fradkin, *Quantum noise and entanglement generated by a local quantum quench*, Phys. Rev. B **80**, 235412 (2009).

[10] H. F. Song, C. Flindt, S. Rachel, I. Klich, and K. Le Hur, *Entanglement from Charge Statistics: Exact Relations for Many-Body Systems*, Phys. Rev. B **83**, 161408(R) (2011).

[11] H. F. Song, S. Rachel, C. Flindt, I. Klich, N. Laflorencie, and K. Le Hur, *Bipartite Fluctuations as a Probe of Many-Body Entanglement*, Phys. Rev. B **85**, 035409 (2012).

[12] P. Calabrese, M. Mintchev and E. Vicari, *Exact relations between particle fluctuations and entanglement in Fermi gases*, EPL **98**, 20003 (2012).

[13] G. C. Levine, M. J. Bantegui, and J. A. Burg, *Full counting statistics in a disordered free fermion system*, Phys. Rev. B **86**, 174202 (2012).

[14] R. Susstrunk and D. A. Ivanov, *Free fermions on a line: Asymptotics of the entanglement entropy and entanglement spectrum from full counting statistics*, EPL **100**, 60009 (2012).

[15] P. Calabrese, P. Le Doussal, and S. N. Majumdar, *Random matrices and entanglement entropy of trapped Fermi gases*, Phys. Rev. A **91**, 012303 (2015).

[16] Y. Utsumi, *Full counting statistics of information content*, Eur. Phys. J. Spec. Top. 227, 1911 (2019).

[17] R. W. Cherng and E. Demler, *Quantum Noise Analysis of Spin Systems Realized with Cold Atoms*, New J. Phys. **9**, 7 (2007).

[18] M. Bortz, J. Sato, and M. Shiroishi M, *String correlation functions of the spin-1/2 Heisenberg XXZ chain*, J. Phys. A **40**, 4253 (2007).

[19] D. B. Abraham, F. H. L. Essler, and A. Maciolek, *Effective Forces Induced by a Fluctuating Interface: Exact Results*, Phys. Rev. Lett. **98**, 170602 (2007).

[20] A. Lamacraft and P. Fendley, *Order Parameter Statistics in the Critical Quantum Ising Chain*, Phys. Rev. Lett. **100**, 165706 (2008).

[21] D. A. Ivanov and A. G. Abanov, *Characterizing correlations with full counting statistics: Classical Ising and quan-*

tum XY spin chains, Phys. Rev. E **87**, 022114 (2013).
[22] Y. Shi and I. Klich, *Full counting statistics and the Edgeworth series for matrix product states*, J. Stat. Mech. (2013) P05001.
[23] V. Eisler, *Universality in the Full Counting Statistics of Trapped Fermions*, Phys. Rev. Lett. 111, 080402 (2013).
[24] I. Klich, *A note on the Full Counting Statistics of paired fermions*, J. Stat. Mech. (2014) P11006.
[25] M. Moreno-Cardoner, J. F. Sherson and G. De Chiara, *Non-Gaussian distribution of collective operators in quantum spin chains*, New J. Phys. **18**, 103015 (2016).
[26] J.-M. Stéphan and F. Pollmann, *Full counting statistics in the Haldane-Shastry chain*, Phys. Rev. B **95**, 035119 (2017).
[27] M. Collura, F. H. L. Essler, and S. Groha, *Full counting statistics in the spin-1/2 Heisenberg XXZ chain*, J. Phys. A **50**, 414002 (2017).
[28] K. Najafi and M. A. Rajabpour, *Full counting statistics of the subsystem energy for free fermions and quantum spin chains*, Phys. Rev. B **96**, 235109 (2017).
[29] S. Humeniuk and H. P. Büchler, *Full Counting Statistics for Interacting Fermions with Determinantal Quantum Monte Carlo Simulations*, Phys. Rev. Lett. **119**, 236401 (2017).
[30] A. Bastianello, L. Piroli, and P. Calabrese, *Exact local correlations and full counting statistics for arbitrary states of the one-dimensional interacting Bose gas*, Phys. Rev. Lett. **120**, 190601 (2018).
[31] A. Bastianello and L. Piroli, *From the sinh-Gordon field theory to the one-dimensional Bose gas: exact local correlations and full counting statistics*, J. Stat. Mech. (2018) 113104.
[32] G. Perfetto, L. Piroli, and Andrea Gambassi, *Quench action and large deviations: Work statistics in the one-dimensional Bose gas*, Phys. Rev. E **100**, 032114 (2019).
[33] V. Gritsev, E. Altman, E. Demler and A. Polkovnikov, *Full quantum distribution of contrast in interference experiments between interacting one-dimensional Bose liquids*, Nature Phys. **2**, 705 (2006).
[34] V. Eisler and Z. Racz, *Full Counting Statistics in a Propagating Quantum Front and Random Matrix Spectra*, Phys. Rev. Lett. **110**, 060602 (2013).
[35] I. Lovas, B. Dora, E. Demler, and G. Zarand, *Full counting statistics of time of flight images*, Phys. Rev. A **95**, 053621 (2017).
[36] S. Groha, F. H. L. Essler, and P. Calabrese, *Full counting statistics in the transverse field Ising chain*, SciPost Phys. **4**, 043 (2018).
[37] M. Collura and F. H. L. Essler, *How order melts after quantum quenches*, Phys. Rev. B **101**, 041110 (2020).
[38] M. Collura, *Relaxation of the order-parameter statistics in the Ising quantum chain*, SciPost Phys. **7**, 072 (2019).
[39] M. Arzamasovs and D. M. Gangardt, *Full Counting Statistics and Large Deviations in a Thermal 1D Bose Gas*, Phys. Rev. Lett. **122**, 120401 (2019).
[40] M. N. Najafi and M. A. Rajabpour, *Formation probabilities and statistics of observables as defect problems in the free fermions and the quantum spin chains*, arXiv:1911.04595.
[41] M. Collura, A. De Luca, P. Calabrese, and J. Dubail, *Domain-wall melting in the spin-1/2 XXZ spin chain: emergent Luttinger liquid with fractal quasi-particle charge*, arXiv:2001.04948
[42] V. Alba, M. Haque, and A. M. Läuchli, *Boundary-Locality and Perturbative Structure of Entanglement Spectra in Gapped Systems*, Phys. Rev. Lett. **108**, 227201 (2012).
[43] I. Peschel, M. Kaulke, and O. Legeza, *Density-matrix spectra for integrable models*, Ann. Physik (Leipzig) **8**, 153 (1999).
[44] P. Calabrese, J. Cardy, and I. Peschel, *Corrections to scaling for block entanglement in massive spin-chains*, J. Stat. Mech. P09003 (2010).
[45] G. Vidal, *Efficient simulation of one-dimensional quantum many-body systems*, Phys. Rev. Lett. **93**, 040502 (2004).
[46] S. Murciano, G. Di Giulio, and P. Calabrese, *Symmetry resolved entanglement in gapped integrable systems: a corner transfer matrix approach*, arXiv:1911.09588.
[47] N. Laflorencie and S. Rachel, *Spin-resolved entanglement spectroscopy of critical spin chains and Luttinger liquids*, J. Stat. Mech. (2014) P11013.
[48] A. Lukin, M. Rispoli, R. Schittko, M. E. Tai, A. M. Kaufman, S. Choi, V. Khemani, J. Leonard, and M. Greiner, *Probing entanglement in a many-body localized system*, Science, **364**, 6437 (2019).
[49] M. Goldstein and E. Sela, *Symmetry-Resolved Entanglement in Many-Body Systems*, Phys. Rev. Lett. **120**, 200602 (2018).
[50] E. Cornfeld, M. Goldstein, and E. Sela, *Imbalance Entanglement: Symmetry Decomposition of Negativity*, Phys. Rev. A **98**, 032302 (2018).
[51] J. C. Xavier, F. C. Alcaraz, and G. Sierra, *Equipartition of the entanglement entropy*, Phys. Rev. B **98**, 041106 (2018).
[52] E. Cornfeld, L. A. Landau, K. Shtengel, and E. Sela, *Entanglement spectroscopy of non-Abelian anyons: Reading off quantum dimensions of individual anyons*, Phys. Rev. B **99**, 115429 (2019).
[53] N. Feldman and M. Goldstein, *Dynamics of Charge-Resolved Entanglement after a Local Quench*, arXiv:1905.10749.
[54] R. Bonsignori, P. Ruggiero and P. Calabrese, *Symmetry resolved entanglement in free fermionic systems*, J. Phys. A **52**, 475302 (2019).
[55] S. Fraenkel and M. Goldstein, *Symmetry resolved entanglement: Exact results in 1D and beyond*, arXiv:1910.08459.
[56] M. T. Tan and S. Ryu, *Particle Number Fluctuations, Rényi and Symmetry-resolved Entanglement Entropy in Two-dimensional Fermi Gas from Multi-dimensional Bosonization*, arXiv:1911.01451.
[57] J. L. Cardy, O. A. Castro-Alvaredo, and B. Doyon, *Form factors of branch-point twist fields in quantum integrable models and entanglement entropy*, J. Stat. Phys. **130**, 129 (2008).
[58] O. A. Castro-Alvaredo and B. Doyon, *Bi-partite entanglement entropy in massive 1+1-dimensional quantum field theories*, J. Phys. A **42**, 504006 (2009).